2019 Rock Dynamics Summit– Aydan et al. (eds)
© 2019 Taylor & Francis Group, London, ISBN 978-0-367-34783-3

Assessment of a complex large slope failure at Kışlaköy open pit mine, Turkey

R. Ulusay
Department of Geological Engineering, Hacettepe University, Ankara, Turkey

Ö. Aydan
Department of Civil Engineering, University of the Ryukyus, Okinawa, Japan

A. Ersen
Ersen Associates, Istanbul, Turkey

ABSTRACT: A very complex slope failure took place at an open-pit coal mine in 1984 in the eastern Turkey. The earlier investigations showed that a basal clay layer at the bottom of the coal seam was the main cause of the failure. The failure took place while the coal seam was uncovered. In this study, a series of back analyses utilizing the information of geotechnical investigations before and after the failure and static and dynamic limiting equilibrium techniques and finite element analyses were performed, and their outcomes are presented and discussed. It is shown that the failure process was complex and involved the buckling of the lignite seam, sliding along the basal clay layer and shearing failure of overburden layers. The drainage conditions also played an important role in the initiation of the failure. Once the failure as initiated, the failure developed rapidly.

1 INTRODUCTION

The failure of slopes during mining operations results in not only loss of the mining machinery but also human lives which make the mining operations become very costly. Therefore, a good design is necessary before the initiation of mining operations since any change of design later on will result in high cost and time loss.

A very complex failure took place at the north-eastern slope of the Kışlaköy open-pit mine of Afşin-Elbistan Lignite Mining Complex in the Eastern Turkey in 1984. The pit-floor heaved up as a result of the buckling failure of the lignite seam and a combined form of shear and sliding failure of mining benches occurred. The investigations showed that weak clay layers existed in the lignite seam of about 20 m thick and one of these clay layers played an important role in the failure (Ulusay et al. 1986).

In this paper, the authors re-consider the 1984 failure from another point of view. Previous analyses for the assessment of stability of these slopes were based on combined failure surfaces partly passing through the slope forming materials and partly along the basal clay layer (Ulusay et al. 1986). Examining the photographs of the failure, the heaved lignite seam shows a set of buckles. Based on this issue, the failure was re-examined by considering also the possibilities of buckling failure and compressive failure of the coal seam which constitutes the pit floor. For this purpose, a series of back analyses utilizing the information of geotechnical investigations before and after the failure, and static and dynamic limiting equilibrium techniques and finite element method were performed. The outcomes of these analyses are presented and discussed.

2 GEOLOGY AND HYDROGEOLOGY

2.1 *Geology*

The Afşin-Elbistan basin is a closed basin and is formed as a result of uplifting of Toros (Taurus) Mountain range at the end of Alps orogenesis. The basin is uplifted and is subjected to a thrust aligned in the direction of NW-SE. There are normal faults, whose strikes are aligned NW-SE and dip to south with an inclination of 70-90°. The orientation of these faults are also indicative of ongoing NW-SE thrust type stress regime (Ketin 1984).

The basal rock unit is limestone of Permo-Carboniferous age (Fig. 1). Both the later units and lignite deposits were formed during the Tertiary period. The deposits above the basal limestone and their characteristics from the bottom to top are briefly described below.

The unit underlaying lignite consists of greenish gray highly plastic clay with some organic content.

Lignite, with a thickness ranging between 10 to 80 m in the pit, is approximately 15-20 m in the location of failure. There are several clayey layers within the lignite seam.

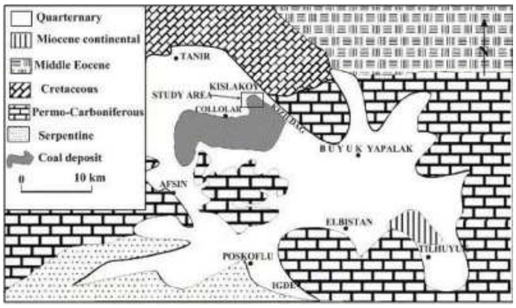

Figure 1. Geology of Afşin-Elbistan basin and location of the Kışlaköy pit (Ural and Yüksel 2004)

Gytja is characterized by a calcereous sandy clayey formation together with remnants of fossils with thickness ranging from a few metres to 50 m and overlies the coal seam. The thickness of this very porous unit is about 0.5-2 m in the failure site.

Blue clay, belonging to Quaternary period, is calcerous unit. It is about 10-15 m thick, dips towards the south with an inclination of 2-4° and has slaking characteristics.

Marl has a grenish colour and a thickness of 0.5-3 m in the failure site.

Loam, which belongs to Quaternary period, is a clayey, sandy and gravelly deposit with a thickness of about 15-40 m. It is a water-bearing porous unit.

2.2 *Hydrogeology*

Loam and gytja deposits are the main water-bearing units. In particular, the porosity and hydraulic conductivity of the gytja is approximately 50 % and about $1{\times}10^{-7}$ m/s, respectively. It is also an artesian in the region. An extensive drainage network has been developed to drain the above these two deposits.

3 DESCRIPTION OF THE FAILURE

The main failure occurred on July 1, 1984 at the North-West slope of the Kışlaköy open-pit mine (Polat and Yüksel 1984). The failure involved a region, which was 650 m long and 250 m wide. The length of the region was later extended to 1000 m with subsequent failures. The final horizontal movement of the failed slope was more than 50 m. The lignite seam of the pit-floor was heaved up and it had a set of buckles whose strikes were almost perpendicular to direction of the movement and parallel to the axis of benches (Fig. 2). Fig. 3 shows the buckled lignite seam in the Kışlaköy open pit.

The first indications of the failure were observed on June 20, 1984 and tension cracks developed behind the slope crest. On June 21, the engineers of the open-pit mine installed gauges to monitor the horizontal and vertical movements of these tension

Figure 2. A view of failed benches in the Kışlaköy open pit

Figure 3. A view of buckled lignite seam in the Kışlaköy open pit mine.

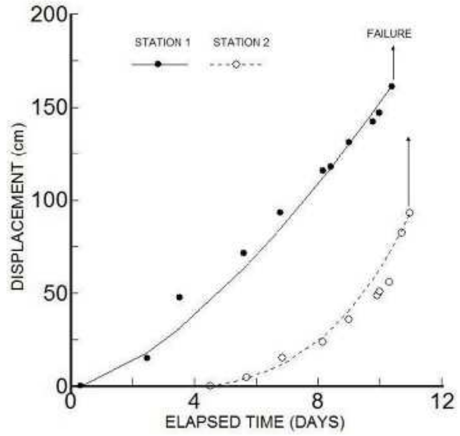

Figure 4. Time-displacement response of monitoring stations at Kışlaköy open pit (arranged from Polat and Yüksel 1984)

cracks. The main tension crack occurred at a distance of 40 m behind the crest of the upper most bench. Fig. 4 shows the vertical movements and associated velocity and acceleration responses as a function of elapsed time at Station 1 (the dynamite depot about 30 m from the slope crest) and Station 2 (a drainage well next to the crest of the upper most bench).

4 GEOMECHANICAL PROPERTIES

Following the failure and concerns about the stability problems on the western slope of the pit near, which the electric power station is situated, an extensive program to investigate geomechanical characteristics of formations for stability analyses was initiated by Ulusay et al. (1986). The shear strength characteristics of the slope forming units are given in Table 1. Their shear responses obtained from direct shear tests are compared with each other in Fig. 5. As seen from the figure, the weak clay has the lowest rigidity and strength while the lignite has the highest rigidity and the strength. On the other hand, blue clay, gytja, marl and loam have similar characteristics.

Table 1. Material properties of the slope forming units (Ulusay et al. 1986; Aydan et al. 1996)

Unit	c_p (kPa)	φ_p (°)	c_r (kPa)	φ_r (°)
Loam	54.0	25.4	38.5	22.9
Marl	51.8	26.8	1.0	25.9
Blue clay	93.0	13.9	78.5	8.9
Gytja	13.5	37.8	9.6	33.5
Weak clay	23.7	2.2	15.5	1.7
Lignite	161.0	33.3	17.9	27.5

c_p, c_r: *Peak and residual cohesion*

φ_p, φ_r: *Peak and residual internal friction angle*

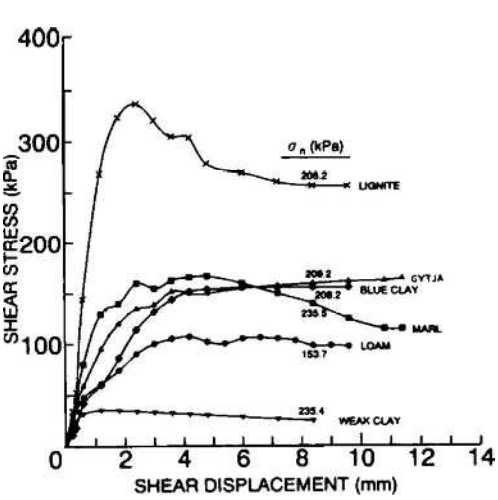

Figure 5. Shear behaviour of the slope forming units.

5 LIMITING EQUILIBRIUM ANALYSES

5.1 *Analyses of the North-West Slope by Conventional Limiting Equilibrium Methods*

First a series of limiting equilibrium analyses were performed by using the Janbu's method (Janbu 1954). The failure surface consisted of two parts: a circular part through loam, marl, blue clay and gytja, and a planar part along the gytja-lignite interface (Fig. 6). All analyses were performed by assuming that the slope was dry in view of the drainage system and in-situ observations. Table 2 gives calculated safety factors for three cross sections shown in Fig. 6 by considering the peak and residual shear strength parameters. The analyses showed that the slope should be stable for these failure surface configurations for both peak and residual values of the strength parameters. The observations on the failure also confirm this conclusion.

A second series of analyses were performed by using the Sarma's method (Sarma 1979). The failure surface passes through a weak clay layer within the lignite seam as shown in Fig. 6. If the peak values are used, the calculated safety factors were again large and the failure was not possible. If the residual values of the strength parameters were used the safety factor was close to 1 or less than that as given

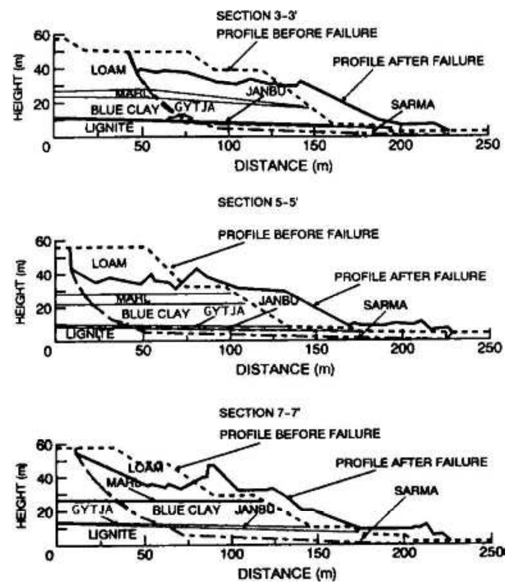

Figure 6. Cross sections used for stability analysis and slope geometries before and after the failure.

Table 2. Safety factors (Janbu's method)

Section	3-3′	5-5′	7-7′
Peak	2.41	2.87	2.18
Residual	1.85	2.26	1.76

Table 3. Safety factors (Sarma's method)

Section	3-3′	5-5′	7-7′
c_r = 11.5 kPa	1.070	1.060	0.980
c_r = 0.0 kPa	1.007	1.002	-

in Table 3. If the residual cohesion of the weak clay was assumed to be nil, the possibility of failure increased. In other words, the failure of the slope was not possible unless residual values were effective and these analyses did not provide any answer to the buckled configuration of the pit-floor. In the next sub-section, an alternative method to analyse the buckling failure is presented.

5.2 *A limiting equilibrium method for a complex shearing, sliding and buckling failure*

Ulusay et al. (1995) proposed a limiting equilibrium analysis method for a failure mechanism shown in Fig. 7. It is assumed that failure takes through shearing of intact layers at the back of the slope and sliding along a bedding plane. For the pit floor layer, there may be two possible modes: MODE 1: compressive failure, and MODE 2: buckling failure, MODE 3: combined compressive and buckling failure.

For the sliding and shearing part, the force system acting on a typical block may be modelled as shown in Fig. 8a. Note that a lateral force is also assumed to act in order to consider the lateral stresses. The

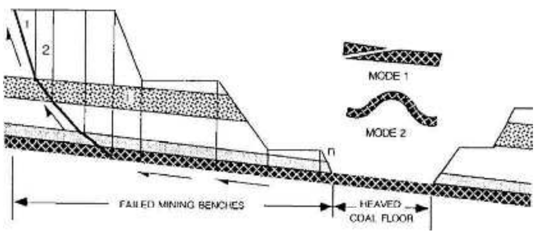

Figure 7. Failure mechanism proposed by Ulusay et al. (1995).

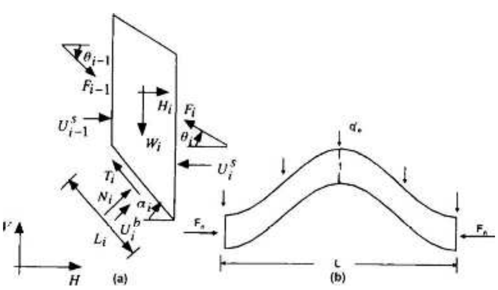

Figure 8. Mechanical models for stability assessment.

equilibrium equations for the chosen coordinate system can be written as:

$$\sum F_s^i = -T_i + W_i \sin\alpha_i + H_i \cos\alpha_i + F_{i-1}\cos(\alpha_i - \theta_{i-1}) -$$

$$F_i \cos(\alpha_i - \theta_i) + (U_{i-1}^s - U_i^s)\cos\alpha_i = 0 \quad (1)$$

$$\sum F_n^i = N_i + U_i^b - W_i \cos\alpha_i + H_i \sin\alpha_i + F_{i-1}\sin(\alpha_i - \theta_{i-1}) -$$

$$F_i \sin(\alpha_i - \theta_i) + (U_{i-1}^s - U_i^s)\sin\alpha_i = 0 \quad (2)$$

Assuming that the rock obeys to the Mohr-Coulomb yield criterion and the ratio of the horizontal force to the weight of the slice is given in the following forms:

$$T_i = \frac{c_i L_i + N_i \tan\varphi_i}{SF}, \quad H_i = \lambda W_i. \quad (3)$$

One easily obtains an equation for inter-slice force F_i, which can be solved *step by step* to obtain the force F_n together with the condition of $F_0 = 0$.

The resistance of the pit floor against compressive failure would be similar to the thrust type faulting. Therefore, no equation is given herein. As for the buckling failure of the coal seam, the following non-homogenous differential equation holds (Fig. 8b):

$$\frac{d^2u}{dx^2} + \frac{F_n}{EI}u = \frac{q_{o'}}{2EI}x(L-x) \quad (4)$$

where E is elastic modulus, I is second areal inertia moment, u is displacement, and $q_{o'}$ is effective distributed load. Solution of the above equation is given below.

$$u = A\cos kx + B\sin kx + \frac{q_{o'}}{4EIk^2}\left(Lx - x^2 + \frac{2}{k^2}\right),$$

$$k^2 = \frac{F_n}{EI} \quad (5)$$

If $u = 0$ and $du/dx = 0$ at the ends of the layer, the integration constants A and B are obtained as follows:

$$A = -\frac{q_{o'}}{F_n k^2}, \quad B = -\frac{q_{o'} L}{F_n k}. \quad (6)$$

Assuming that $du/dx = 0$ at $x = L/2$, the critical buckling load is obtained as:

$$F_n = EI\left(\frac{8.99}{L}\right)^2 \quad (7)$$

Introducing $I = bt^3/12$ and $F_n = \sigma_o bt$, the critical axial stress for buckling is obtained as follows

$$\sigma_o^{cr} = 6.735E\left(\frac{t}{L}\right)^2 \quad (8)$$

where t is layer thickness, and L is span. An application of the above approach is shown in Fig. 9. Fig 9a was obtained from force $F_n = \sigma_o bt$ by considering the combined shearing and sliding failure for $SF = 1$ by varying lateral stress coefficient λ.

Fig. 9b was obtained from buckling analysis by assuming that E / σ_c as 65 (continuous line) and 26 (broken line). Since it is more likely that the peak strength values hold, the slope may become unstable and pit floor fails in compression provided that the lateral stress coefficient is 0.13 for a uniaxial strength of 596 kPa. As for buckling failure, the lateral stress coefficient failure should be greater than 0.1 and less than 0.13 in view of the actual range of L / t at the time of failure. The uncovered span of the lignite seam was 113 m at the time of failure. If the thin *Gytja* formation just above the lignite seam near the toe of the slope is neglected, the effective span is about 153 m. For a 5 m thick lignite seam, the value of L / t for compressive failure is found to be 21.95 from Fig. 9b. If the effect of the Gytja formation on L / t ratio is taken into account, the L / t is 22.6. On the other hand, if its effect is neglected, L / t is 30.6. Considering the above numbers, it has been contemplated that the lignite seam would likely be buckling rather than failing in compression. If the thickness of the seam involved in failure is thinner than 5 m, the possibility of failure by buckling increases more rapidly as compared with that by compression.

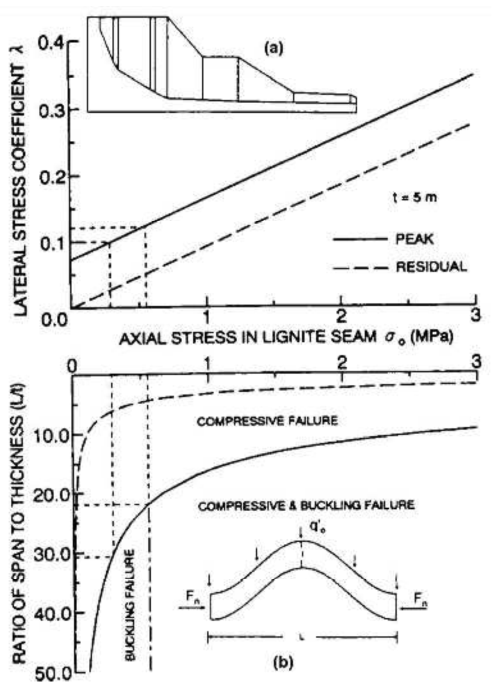

Figure 9. Computed stability chart for the lignite seam.

6 FINITE ELEMENT ANALYSES

The discrete finite element method proposed by Aydan-Mamaghani (Aydan et al. 1996(a,b); Mamaghani et al. 1994) was chosen to simulate the failure process of the slope . This method is based entirely on finite element method and can simulate very large deformation of jointed media. Material properties used in the analyses are given in Table 4. Fig. 10 shows the finite element mesh and boundary conditions.

First, a series of elastic analyses was carried out by varying lateral stress coefficient κ to see the magnitude of the axial stress of lignite seam at the location adjacent to the sliding benches. Fig. 11 shows the relation between lateral stress coefficient κ and the axial stress in lignite seam. As seen from the figure, lateral stress coefficient must be greater than 0.58 and less than 0.78 to cause the buckling of the seam. Otherwise, the lignite seam must fail in compression which is contradictory against field evidents. The results further indicates that if the lateral stress coefficient is less than 0.58, the axial stress in the seam may be tensile. By setting the lateral stress coefficient κ as 0.7, an elasto-plastic analysis was carried out. Fig. 12 shows the deformed configuration of the open-pit for each respective pseudo time step. As seen from this figure, the sliding of the benches on the left-hand side and buckling of the lignite seam at pit-floor are well simulated.

Table 4. Geomechanical parameters used in DFEM analysis.

Unit	λ (MPa)	μ (MPa)	c (kPa)	φ (°)
Loam, Marl, Blue clay	408	5.4	60	25
Lignite	710	9.4	161	33
Base layer	670	38	161	33
Weak clay	3.2	1.1	23	6
Fracture plane	3.2	1.1	23	20

λ, μ:Lame coefficients; c: Cohesion; ϕ : Internal friction angle

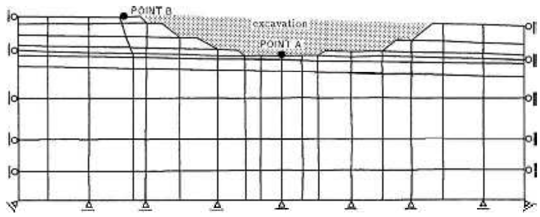

Figure 10. Finite element mesh used in analyses.

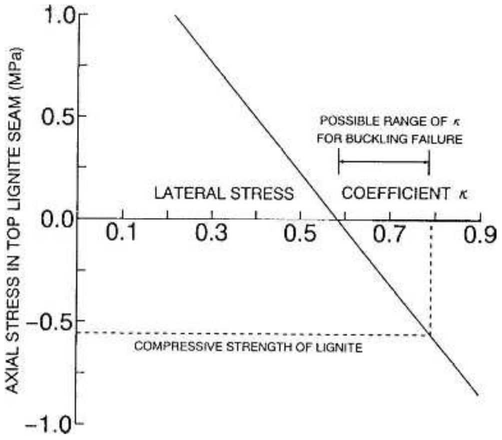

Figure 11. Computed stability chart for buckling failure.

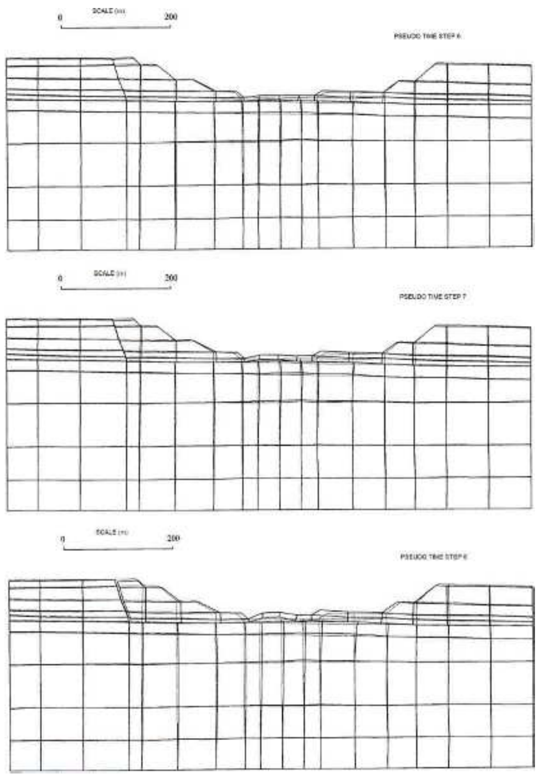

Figure 12. Deformed configurations at various pseudo time steps.

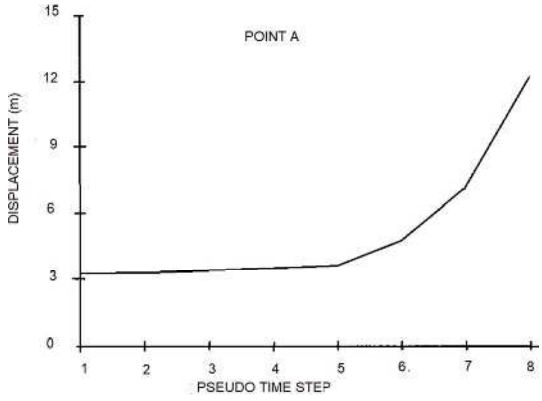

Figure 13 Pseudo time step vs displacement for point A.

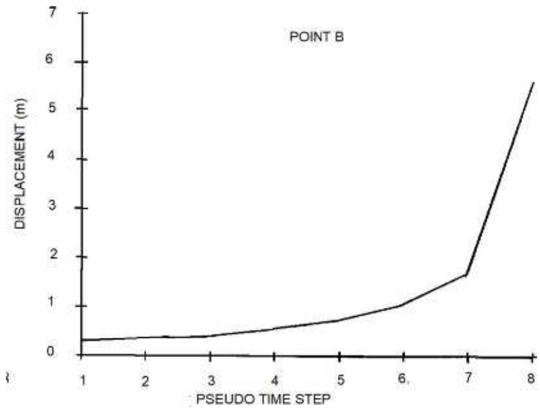

Figure 14 Pseudo time step vs displacement for point B.

It should be noted if the analysis becomes non-convergent in finite element analysis, this may be taken as the indication of failure of the structure, and each iteration step can be regarded as pseudo time step. With this concept in mind, the displacement responses of open-pit at selected point shown in Fig. 12 are plotted in Figs. 13 and 14. The displacement response of point A which is located at the center of the pit-floor corresponds to the heaving of the floor. The heaving of the floor proceeds at a constant rate up to pseudo time step 6 and thereafter increases with an increasing rate and the floor buckles.

The displacement response of point B which is selected at the rear top of the sliding benches corresponds to the horizontal displacement of the sliding body. This response is very similar to the measured response shown in Fig. 4.

7 DYNAMIC LIMITING EQUILIBRIUM METHOD

The method used for estimating post-failure motions of the failed body is based on the earlier proposals by Aydan et al. (2006, 2008), Aydan and Ulusay (2002) and Tokashiki and Aydan (2011). Let us consider a landslide body consisting of N number of blocks sliding on a slip surface as shown in Fig. 15. If inter-slice forces are chosen to be nil as assumed in the simple sliding model (Fellenius-type), one may write the following equation of motion for the sliding body

$$\sum_{i=1}^{n}(S_i - T_i) = \bar{m}\frac{d^2 s}{dt^2} \quad (9)$$

where $\bar{m}, s, t, n$, S_i and T_i are total mass, travel distance, time, number of slices, shear force and shear resistance, respectively. Shear force and shear resistance may be given in the following forms together with Bingham-type yield criterion:

$$S_i = W_i(1+\frac{a_H}{g})\sin\alpha_i;$$

$$T_i = c_i A_i + (N_i - U_i)\tan\varphi_i + \eta W_i\left(\frac{ds_i}{dt}\right)^b \quad (10)$$

where $W_i, A_i, N_i, U_i, \alpha_i, a_V, a_H, c_i, \varphi_i, \eta$ and b are weight, basal area, normal force, uplift pore water force, basal inclination, vertical and horizontal earthquake acceleration, cohesion, friction angle of slice i, Bingham type viscosity and empirical coefficient, respectively. If normal force and pore water uplift force related to the weight of each block as given below

$$N_i = W_i(1+\frac{a_V}{g})\cos\alpha_i \;\; U_i = r_u W_i \quad (11)$$

One can easily derive the following differential equation with the use of Eqs. 9-11:

$$\frac{d^2 s}{dt^2} + \eta\left(\frac{ds}{dt}\right)^b - B(t) = 0 \quad (12)$$

where

$$B(t) = \frac{g}{\bar{m}}\left(\sum_{i=1}^{n} m_i\left((\sin\alpha_i(1+\frac{a_H}{g})\right.\right.$$

$$\left.\left.(\cos\alpha_i(1+\frac{a_V}{g}) - r_u)\tan\varphi_i\right) + \frac{c_i A_i}{g}\right) \quad (13)$$

In the derivation of Eq. (12), the viscous resistance of shear plane of each block is related to the overall viscous resistance in the following form:

$$\eta\bar{m}g\left(\frac{ds}{dt}\right)^b = \sum_{i=1}^{n}\eta m_i g\left(\frac{ds_i}{dt}\right)^b \quad (14)$$

Eq. (12) can be solved for the following initial conditions together with the definition of the geometry of basal slip plane.

At time $t = t_o$ (15)

$s = s_o$ and $v = v_o$

There may be different forms of constitutive laws for the slip surface (i.e. Aydan et al. 2006, 2008; Aydan and Ulusay, 2002). The simplest model would be elastic-brittle plastic to implement. If this model is adopted, the cohesion will exist at the start of motion and it will disappear thereafter. Therefore, cohesion component introduced in Eq. (13) may be taken as nil as soon as the motion starts. Thereafter, the shear resistance will consist of mainly frictional component together with some viscous resistance.

The method explained above was applied by Tokashiki and Aydan (2011) to Kita-Uebaru landslide in Okinawa (Japan) involving bedding plane and fault plane. This method utilizes Bingham type visco-plastic yield criterion. Although the assumed geometry of the open-pit mine is slightly different from the actual one, it was applied to the failure in the Kışlaköy open-pit mine. Fig. 16 shows the displacement response during failure. The actual displacement of the failed body was about 34 m. The estimated displacement of the failed body is about 33 m. The material properties are shown in Figs. 16 and 17, which are based on those given in Table 4. Fig. 17 shows the deformation configuration of the failed body in space with time. Despite some

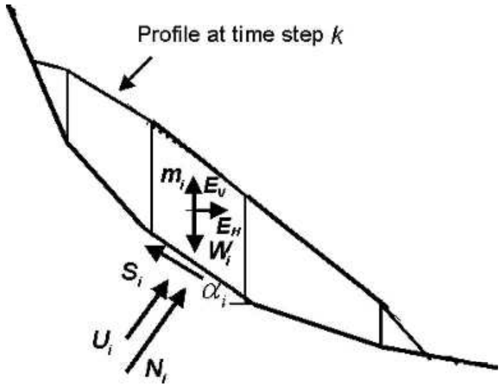

Figure 15 Mechanical model for estimating post-failure motions (Aydan 2016).

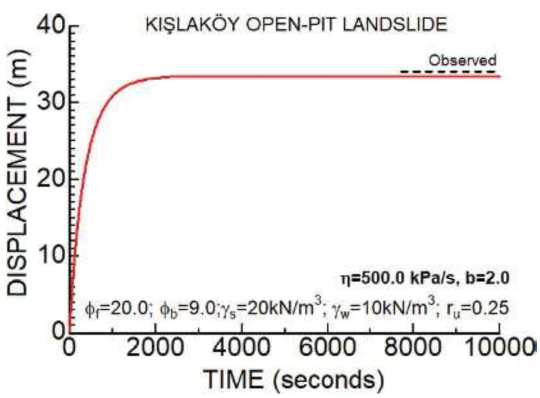

Figure 16. Displacement response of the mass center of the failed body.

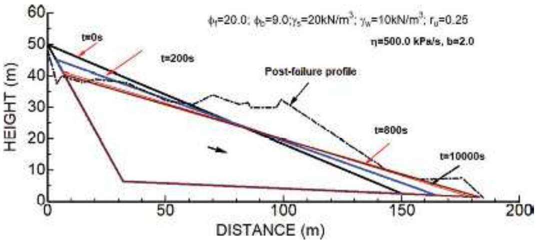

Figure. 17. Deformed configurations of the failed body.

difference between the assumed and actual geometries of the failed body, the estimations are very close to the actual ones.

8 CONCLUSIONS

From the back analyses of the failed slope, the following conclusions may be drawn.

The existence of a weak clay layer within the lignite seam with a very low shear modulus and strength played an important role and caused very high compressive stresses in the lignite seam.

The stresses are further increased by thinning the overlaying layers because of the excavation.

The failure of slope is not possible unless the residual values are utilised which is very unrealistic in limiting equilibrium analyses. If the effect of lateral force is taken into account, the failure becomes possible, provided that the lateral force coefficient is greater than 0.1 in view of the actual span of the lignite seam at the time of failure. The lateral force coefficient is likely to be greater than 0.1, if the stress regime of the region is taken into account.

Finite element computations showed that the buckling failure of the pit-floor was possible when the lateral in-situ stress coefficient was between 0.58 and 0.78. The computed responses were very similar to those measured.

Dynamic limiting equilibirum appraoch was also applied to estimate the post-failure motions of the open-pit failure and the estimations were very close to the actual observations.

In the same open-pit, there were failures at the east slope in 1988 when the depth of excavation was almost the same as the one reported herein. A series of in-situ measurements on the stress state of the region is needed for a better design of future open-pits at the Afşin-Elbistan Mining Complex.

REFERENCES

Aydan, Ö., 2016. Some considerations on a large landslide at the left bank of the Aratozawa Dam caused by the 2008 Iwate-Miyagi intraplate earthquake, Rock Mechanics and Rock Engineering, Special Issue on Deep-seated Landslides. 49(6):2525–2539,

Aydan, Ö., Ulusay, R., 2002. A back analysis of the failure of a highway embankment at Bakacak during the 1999Düzce-Bolu earthquake. Env. Geol. 42: 621–631.

Aydan, Ö., Ulusay, R., Kumsar, H., Ersen, A. 1996a. Buckling failure at an open-pit coal mine. EUROCK96, 641–648.

Aydan, Ö., Mamaghani, I.H.P., Kawamoto, T. 1996b. Application of dicrete finite element method (DFEM) to rock engineering structures. NARMS'96, Montreal.

Aydan, Ö., Daido, M., Ito, T., Tano, H. and Kawamoto, T. 2006. Prediction of post-failure motions of rock slopes induced by earthquakes. 4th Asian Rock Mechanics Symposium, Singapore, Paper No. A0356 (on CD).

Aydan, Ö., Ulusay R., Atak, V.O. 2008. Evaluation of ground deformations induced by the 1999 Kocaeli earthquake (Turkey) at selected sites on shorelines. Environmental Geology, Springer Verlag, 54, 165–182.

Janbu, N. 1954. Application of composite slip circles for stability analysis. European Conf. on Stability of Earth Slopes, Stockholm, 3:43–49.

Ketin, I., 1984. A general view to geology of Turkey. ITU Vakfı Yayını, No.32, İstanbul (in Turkish).

Mamaghani, I.H.P, Baba, S., Aydan, Ö., Shimizu, Y. 1994. Dicrete finite element method for blocky systems. IACMAG, 843–850.

Polat, H. Yüksel, M.F. 1984. Geology and cuases of the landslide area. Report of Geology Division of TKI-AEL, 55 (in Turkish, unpublished).

Sarma, S.K. 1979. Stability analysis of embankments and slopes. J. Geotech. Div., ASCE, 105(12):1511–1524.

Tokashiki, N. Aydan, Ö. 2011. Kita-Uebaru natural rock slope failure and its back analysis. Environmental Earth Sciences, 62 (1): 25–31.

Ulusay, R., Koçak, S., Selçuk, S., Ider, M.H. 1986. Stability of the West slope of Kışlaköy (Elbistan-K.Maraş) open pit. Proc. of the 1st Rock Mechanics Symposium, Turksih National Soceiety for Rock Mechanics, Ankara, 467–487 (in Turkish).

Ulusay, R., Aydan, Ö., Karaca, M. and Ersen, A. 1995. Buckling failure of an open-pit mine and its back analyses. Proc. of the 8th Int. Rock Mech. Symp., Tokyo, 451–454.

Ural, S. Yüksel, F. 2004. Geotechnical characterization of lignite-bearing horizons in the Afsin–Elbistan lignite basin, SE Turkey. Engineering Geology, 75 (2): 129–146.